J Solid State Electrochem (2012) 16:1889–1892
DOI 10.1007/s10008-011-1466-9

ORIGINAL PAPER

Graphene anchored with mesoporous NiO nanoplates as anode material for lithium-ion batteries

Danfeng Qiu · Zijing Xu · Mingbo Zheng · Bin Zhao · Lijia Pan · Lin Pu · Yi Shi

Received: 15 April 2011 / Revised: 31 May 2011 / Accepted: 7 June 2011 / Published online: 18 June 2011

Abstract Graphene is an excellent substrate to load nanomaterials for energy applications due to its large surface area, excellent conductivity, mechanical strength, and chemical stability. In this study, thermal exfoliated functionalized graphene sheets with good conductivity and high BET surface area are anchored with mesoporous NiO nanoplates by in situ chemical synthesis approach. Electrochemical characterization shows that functionalized graphene sheets–NiO sample exhibits a high capacity of about 700 mAh/g at a discharge current density of 100 mA/g and a good cycling ability. The high capacity and good cycling ability of functionalized graphene sheets –NiO material were attributed to the intimate interaction between the graphene sheets and NiO nanoplates. The graphene sheets not only enhance the conductivity of NiO nanoplates but also improve the structure stability of NiO nanoplates. Furthermore, the mesoporous structure of NiO nanoplates is available to the transfer of electrolyte. Such functionalized graphene sheets–NiO nanocomposite could be a promising candidate material for a high-capacity, low cost, and nontoxic anode for lithium-ion batteries.

Keywords NiO nanoplates · Graphene · Mesoporous · Lithium-ion batteries

Abbreviation
FGS Functionalized graphene sheets

Danfeng Qiu and Zijing Xu contributed equally to this work.

D. Qiu · Z. Xu · M. Zheng (✉) · B. Zhao · L. Pan · L. Pu · Y. Shi
National Laboratory of Microstructures,
School of Electronic Science and Engineering, Nanjing University,
Nanjing 210093, China
e-mail: zhengmingbo@nju.edu.cn

Y. Shi
e-mail: yshi@nju.edu.cn

Introduction

Rechargeable solid-state batteries have long been considered an attractive power source for a wide variety of applications. Among those new technologies, lithium-ion batteries (LIBs) are the technology of choice for portable, entertainment, computing, and telecommunication equipment in today's information-rich, mobile society [1–3]. Finding new electrode materials with higher energy density or better capacity retention or faster charge/discharge rate has been one of the most important research focuses. Nanoparticles of transition-metal oxides, such as Co_3O_4 [4], SnO_2 [5], Fe_2O_3 [6], and NiO [7], have long been considered as anode materials for LIBs because of their higher theoretical capacities than graphite [8]. Among those materials, NiO attracts extensive interest for LIBs due to its low price, nontoxic, and high theoretical capacity. However, due to its low ionic and electronic conductivity, NiO shows poor circle performances as well as slow charge/discharge rate, which limits its further application.

Graphene is an excellent substrate to host active nanomaterials for energy applications due to its high conductivity, large surface area, flexibility, mechanical strength, light weight, and chemical stability [9]. In this study, thermal exfoliated functionalized graphene sheets (FGS) [10] with good conductivity and high BET surface area are anchored with mesoporous NiO nanoplates. Electrochemical characterization shows that FGS/NiO sample exhibits a high capacity of about 700 mAh/g at a discharge current density of 100 mA/g and a good cycling ability. When the current density is increased to 400 mA/g, more than 70% of the capacity can be retained. Such growth-on-graphene approach greatly enhances the cycle performance of the electrode material with poor conductivity.

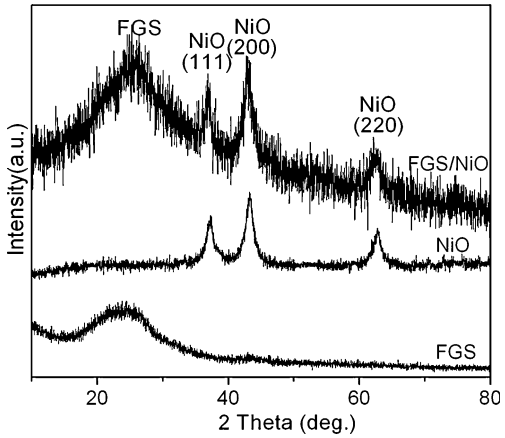

Fig. 1 XRD patterns of FGS, NiO, and FGS/NiO nanocomposite

Experimental

Graphite oxide (GO) was synthesized from natural graphite powders (universal grade, 99.985%) according to a modified Hummers' method [11, 12]. The dried GO was thermally exfoliated at 300 °C for 3 min under air atmosphere, and then it was subsequently treated at 900 °C in Ar for 3 h with a heating rate of 2 °C/min. The obtained samples were denoted as FGS [10].

In a typical synthesis of FGS/NiO composite, as-synthesized FGS (44 mg) was firstly suspended in an aqueous solution containing NaOH (40 mg) and Ni $(NO_3)_2 \cdot 6H_2O$ (290.8 mg) dissolved in 70 mL distilled water, and then ultrasonically treated for 10 min, followed by a hydrothermal treatment at 180 °C for 18 h. The product ($FGS/Ni(OH)_2$) was collected by centrifuging, water washing, and ethanol washing. Then it was subsequently treated at 250 °C in Ar for 3 h with a heating rate of 2 °C/min and the mechanism can be illustrated by following equations: $Ni(OH)_2 \rightarrow NiO + H_2O$. And the NiO content in FGS/NiO composite was ~50% by weight.

The FGS/NiO active material powder (~100 mg) was mixed with polyvinyldifluoride, with weight ratio of 90:10,

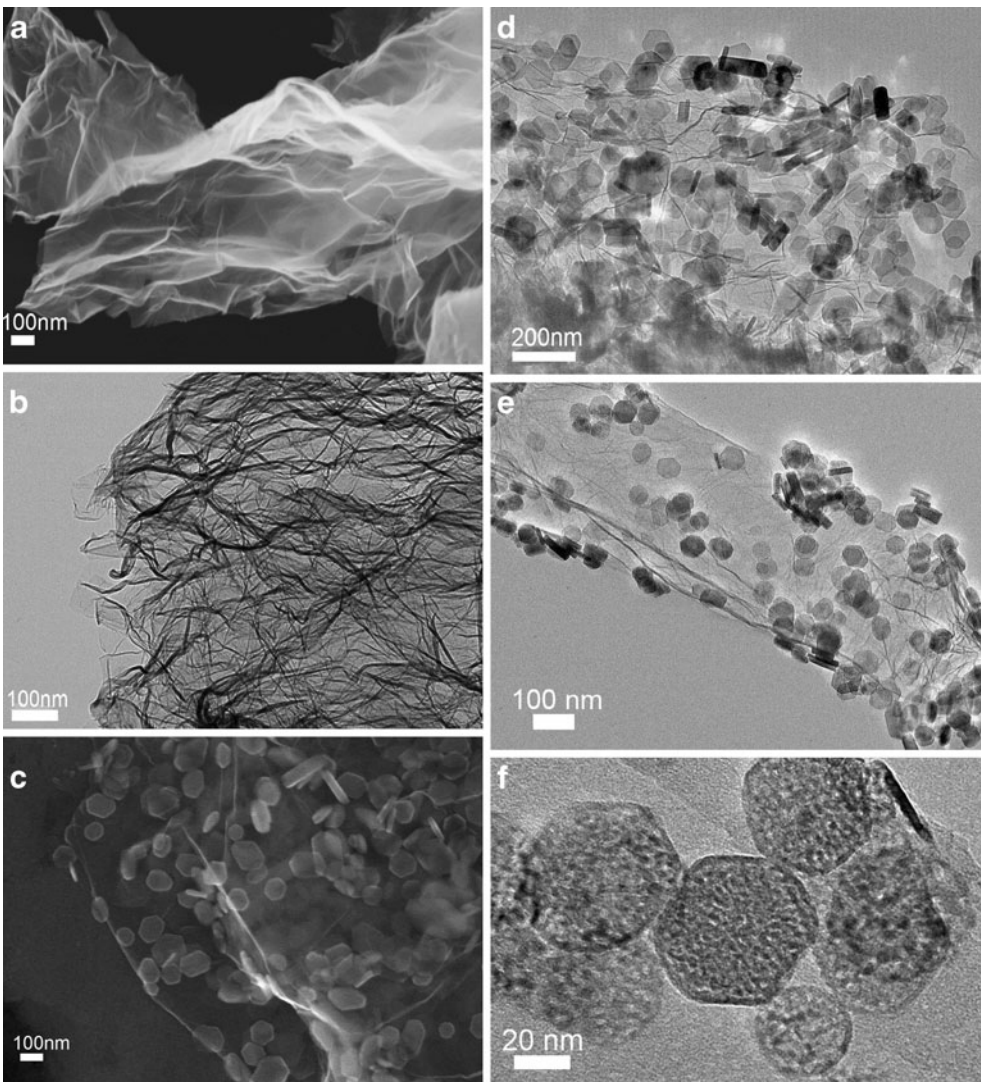

Fig. 2 **a** SEM image of FGS, **b** TEM image of FGS, **c** SEM image of $FGS/Ni(OH)_2$ nanocomposite, **d** TEM image of $FGS/Ni(OH)_2$ nanocomposite, **e** TEM image of FGS/NiO nanocomposite, and **f** high-resolution TEM image of FGS/NiO nanocomposite

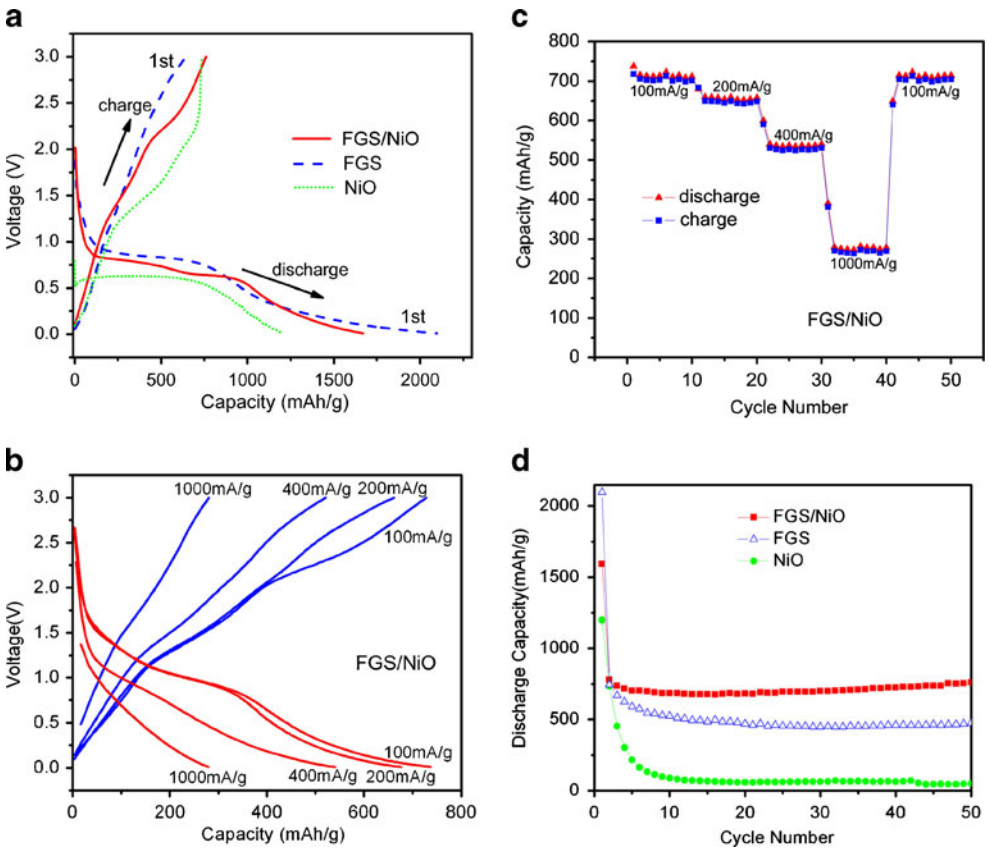

Fig. 3 Electrochemical characterizations for FGS, NiO nanoplates, and FGS/NiO nanocomposite. **a** First discharge and charge curves of FGS/NiO (*red*), FGS (*blue*), and NiO (*green*) at a current density of 100 mA/g. **b** Representative charge (*blue*) and discharge (*red*) curves of FGS/NiO at various current densities. **c** Capacity retention of FGS/NiO at various current densities. **d** Discharge capacity retention of FGS/NiO (*red*), FGS (*blue*), and NiO (*green*) at a current density of 100 mA/g

in *N*-methylpyrrolidone solvent to produce electrode slurry. The slurry was coated onto a copper foil current collector using doctor-blading method [13] and then dried in vacuum and weighed about 2 mg/cm^2. Coin cells were assembled in a glove box filled with argon atmosphere. Test cells were assembled into CR2032-type coin cells composed of FGS/NiO working electrode, Celgard separator, and Li metal foil. The electrolyte was 1 M LiPF6 in ethylene carbonate and diethyl carbonate (1:1 vol). These test cells were then galvanostatically swept at a voltage in the range of 0.01–3 V referred to the Li/Li$^+$ electrode potential.

Results and discussion

Figure 1 shows the XRD patterns of FGS, NiO nanoplates, and FGS/NiO composites. Diffraction peaks at 37.2°, 43.2°, and 62.8° can be indexed to the (111), (200), and (220) planes of cubic-phased NiO, respectively. The broad peak at about 25° was the diffraction peak from the multilayer graphene of FGS sample. Figure 2a, b shows the SEM and TEM images of FGS. The FGS sample has a nanosheet structure, which results from the decomposition of the oxygen-containing groups of GO during the thermal exfoliation process [10]. Figure 2c, d shows the typical SEM and TEM images of FGS/Ni(OH)$_2$. The side length of the Ni(OH)$_2$ nanoplates was about 100 nm, and the thickness was about tens of nanometers. The nanoplates connect tightly with the graphene sheets. Figure 2e, f indicates that NiO retains the nanoplate structure after the heat treatment and possesses mesoporous structure. The dehydration of Ni(OH)$_2$ during the heat treatment results in the formation of mesopores.

Figure 3a shows the first discharge and charge curves of FGS/NiO, FGS, and NiO at a current density of 100 mA/g and measured between 3.0 and 0.01 V vs Li$^+$/Li. The first discharge curve of FGS shows that FGS has a voltage plateau at about 0.84 V. Furthermore, the first discharge curve of NiO indicates that NiO has a voltage plateau at about 0.64 V. For FGS/NiO, in the first discharge, there is a quick potential drop to about 0.84 V at first, followed by a long voltage plateau between 0.84 and 0.6 V. This voltage plateau is from two kinds of reactions. One is from the convention reaction of NiO [14]: NiO + 2Li↔Ni + Li$_2$O.

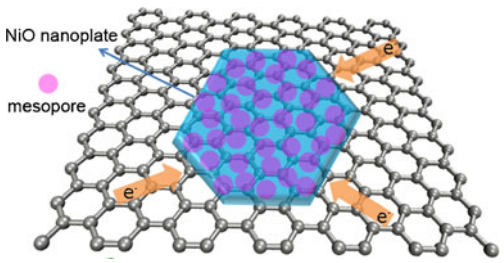

Fig. 4 Schematic illustration of the FGS/NiO nanocomposite

The other is from the reaction of FGS with Li. The sloping part at the end of the discharge curve between 0.6 and 0.01 V could be attributed to the formation of a solid electrolyte interface (SEI) film and the reversible reaction between lithium and graphene sheets $2C + Li^+ + e^- \leftrightarrow LiC_2$. The first discharge and charge capacities for FGS/NiO electrode are about 1,650 and 750 mAh/g. The initial capacity loss may result from the formation of SEI film [15] and the reaction of oxygen-containing functional groups on graphene with lithium ions [16, 17]. The first charge curve of FGS/NiO exhibits two sloping potential ranges at about 1.5 and 2.25 V [18], respectively.

Figure 3b shows representative charge and discharge curves of FGS/NiO at various current densities. With the increase of current density, the charge potential of FGS/NiO increased and the discharge potential decreased, rendering higher overpotential. The cell was first cycled at a low current density of 100 mA/g for 10 cycles, where a stable specific capacity of about 700 mAh/g (Fig. 3c) was obtained. The capacity was as high as 520 mAh/g after the current density was increased by four times, still higher than the theoretical capacity of graphite (372 mAh/g). Even at a high current density of 1,000 mA/g, more than 35% of the capacity can be retained. A capacity of about 700 mAh/g was retained after 50 cycles of charge and discharge at various current densities (Fig. 3c), indicating good cycling stability.

In a control experiment, NiO nanoplates were synthesized by the same method without any graphene added. The electrochemical performance of these NiO nanoplates physically mixed with carbon black was much worse than that of FGS/NiO nanocomposite. At a low current density of 100 mA/g, FGS electrode exhibited good cycle performance but showed a capacity lower than that of FGS/NiO nanocomposite. FGS/NiO nanocomposite showed a capacity of about 700 mAh/g even after 50 cycles, while the capacity of NiO nanoplates decreased to about 100 mAh/g after only 10 cycles (Fig. 3d). The FGS/NiO nanocomposite electrode demonstrated much better electrochemical performance than that of the single NiO electrode.

Figure 4 schematically illustrates the typical structure of NiO nanoplate–FGS nanocomposite material. FGS is an attractive material for combination with poor conductive electrode materials because it ensures a fast electron conduction path and a nanosize framework for loading materials resulting in improved electrochemical performance [13, 19]. The high capacity, good rate capability, and good cycling stability of FGS/NiO nanocomposite material were attributed to the intimate interaction between the graphene substrates and the mesoporous NiO nanoplates. The intimate interaction makes NiO electrochemically active since charge carriers could be effectively and rapidly conducted back and forth from the NiO nanoplates to the current collector through the highly conducting three-dimensional functional graphene sheets network. Furthermore, the mesoporous structure of NiO nanoplates is available to the transfer of electrolyte during the charge–discharge process.

Conclusion

In summary, we have synthesized a novel NiO nanoplate–FGS nanocomposite as the anode material for lithium-ion batteries. The flexible graphene sheets provide high electrical conductivity throughout the electrode and serve as a mechanically strong framework. As a result, this flexible composite structure offers great advantages to enhance the lithium storage capacity, cyclic stability, and rate capability, indicating its promising potential for use as a novel anode material for high-performance LIBs.

Acknowledgments This work was supported by China Postdoctoral Science Foundation (No. 20100471296), Postdoctoral Foundation of Jiangsu Province (No. 1001003C), Nature Science Foundation of Jiangsu Province (No. BK2007146), and National Nature Science Foundation of China (No. 60928009 and 60990314).

Reference

1. Armand M, Tarascon JM (2008) Nature 451:652–657
2. Ellis BL, Lee KT, Nazar LF (2010) Chem Mater 22:691–714
3. Scrosati B, Garche J (2010) J Power Sources 195:2419–2430
4. Li WY, Xu LN, Chen J (2005) Adv Funct Mater 15:851–857
5. Meduri P, Pendyala C, Kumar V, Sumanasekera GU, Sunkara MK (2009) Nano Lett 9:612–616
6. Wu CZ, Yin P, Zhu X, Yang CZO, Xie Y (2006) J Phys Chem B 110:17806–17812
7. Varghese B, Reddy MV, Wu ZY, Lit CS, Rao HTC, Chowdari BV, Wee ATS, Lim CT, Sow CH (2008) Chem Mater 20:3360–3367
8. Boukamp BA, Lesh GC, Huggins RA (1981) J Electrochem Soc 128:725–730
9. Wang HL, Casalongue HS, Liang YY, Dai HJ (2010) J Am Chem Soc 132:7472–7477
10. Du QL, Zheng MB, Zhang LF, Wang YW, Chen JH, Xue LP, Dai WJ, Ji GB, Cao JM (2010) Electrochim Acta 55:3897–3903
11. Hummers WS, Offeman RE (1958) J Am Chem Soc 80:1339–1339
12. Liu PG, Gong KC, Xiao P, Xiao M (2000) J Mater Chem 10:933–935
13. Howatt G, Breckenridge R, Brownlow J (1947) J Am Ceram Soc 30:237–242
14. Huang XH, Tu JP, Zhang CQ, Zhou F (2010) Electrochim Acta 16:8981–8985
15. Derrien G, Hassoun J, Panero S, Scrosati B (2007) Adv Mater 19:2336–2340
16. Ban CM, Wu ZC, Gillaspie DT, Chen L, Yan YF, Blackburn JL, Dillon AC (2010) Adv Mater 22:E145–E149
17. Guo P, Song HH, Chen XH (2009) Electrochem Commun 11:1320–1324
18. Rahman MM, Chou SL, Zhong C, Wang JZ, Wexler D, Liu HK (2010) Solid State Ionics 180:1646–1651
19. Zhou GM, Wang DW, Li F, Zhang LL, Li N, Wu ZS, Wen L, Lu GQ, Cheng HM (2010) Chem Mater 22:5306–5313